Structure of the Atlantic Ocean Equatorial Deep Jets*

GREGORY C. JOHNSON

NOAA/Pacific Marine Environmental Laboratory, Seattle, Washington

DONGXIAO ZHANG

Joint Institute for the Study of the Atmosphere and Ocean, University of Washington, Seattle, Washington

(Manuscript received 25 May 2002, in final form 13 September 2002)

ABSTRACT

The equatorial deep jets in the Atlantic Ocean are described using vertical strain, ξ_z, estimated from all available deep CTD stations in the region. Wavelet analysis reveals a distinct energy peak around 661-sdbar vertical wavelength, 1232-dbar pressure, and $\pm 1.5°$ latitude from the equator. This high-vertical-wavenumber and off-equatorial maximum, coupled with previously published velocity data that show nodes in zonal velocity near $\pm 1.5°$, is grossly consistent with the structure of first-meridional-mode equatorial Rossby waves. However, the meridional scale obtained from the observations exceeds, by about 1.5, the theoretical meridional scale for these waves. The jets are strong, with zonal velocities similar in magnitude to the Kelvin wave phase speed for their vertical wavelength. Harmonics of ξ_z at vertical wavelengths of 1/2, 1/4, and perhaps 1/8 that of the primary peak provide evidence of a large-amplitude structure. Although sparse, available phase data at the 661-sdbar vertical wavelength suggest downward and westward phase propagation. Assuming sinusoidal character in time and longitude gives estimates of a 5- (± 1) yr period and a 70° ($\pm 60°$) zonal wavelength. These vertical, temporal, and zonal scales are roughly consistent with first-meridional-mode equatorial Rossby wave dynamics. However, although vertical and zonal phase propagation are discernible, there is no obvious signature of upward energy propagation in the variance vertical maxima, which is problematic for a simple linear Rossby wave interpretation.

1. Introduction

Equatorial deep jets (EDJs) are equatorially trapped features with short vertical scales that are found in all three oceans. In the Pacific they have been shown to have very long timescales and zonal scales (Johnson et al. 2002). Here the EDJs are analyzed in the Atlantic Ocean using profiles of vertical strain ξ_z estimated from all publicly available CTD station data, also finding long timescales and zonal scales. Vertical stretching and squashing of the density field is revealed by ξ_z, which is closely related to vertical stratification. Using ξ_z instead of the more commonly employed vertical displacement (Eriksen 1982) reduces noise from salinity calibration offsets. This substitution allows use of CTD data from many different sources without undue introduction of error.

Previous observational work on the Atlantic EDJs is reviewed in section 1. The CTD data publicly available in the equatorial Atlantic are described and their processing is detailed in section 2. A qualitative look at the meridional structure of the EDJs in ξ_z is given in section 3. Wavelet analysis of the EDJs allows quantitative estimates of the EDJ structure, including vertical wavelength, meridional structure, timescales, and zonal scales in section 4. The results and their implications for EDJ dynamics are discussed in section 5.

EDJ-like signatures in zonal velocity data from three 6-month deployments of deep current meter moorings in the eastern Atlantic included vertical scales of several hundred meters and timescales of at least several months (Weisberg and Horigan 1981). These signatures were argued to be most consistent with long Rossby waves, and the likelihood of nonlinearity was noted because zonal velocities and phase speeds were comparable. Geostrophic signatures of the EDJs in the western Atlantic Ocean were estimated from analysis of vertical displacement spectra from 1972 Geochemical Ocean Sections Study (GEOSECS) CTD data along 36°W (Eriksen 1982). The conclusion from that analysis was that near-equatorial maxima in the spectra at several-hundred-meter vertical wavelengths were consistent with Kelvin wave dynamics. However, sparse sampling

* Pacific Marine Environmental Laboratory Contribution Number 2475 and Joint Institute for the Study of the Atmosphere and Ocean Contribution Number 933.

Corresponding author address: Dr. Gregory C. Johnson, NOAA/Pacific Marine Environmental Laboratory, 7600 Sand Point Way N.E., Bldg. 3, Seattle, WA 98115-6349.
E-mail: gjohnson@pmel.noaa.gov

makes this conclusion tentative. A single vertical profile of zonal velocity taken on the equator at 30°W in January of 1989 (Ponte et al. 1990) showed the EDJs in the upper 2500 m, with vertical scales of several hundred meters and a particularly prominent eastward jet near 1000-m depth. Another profile taken at the same location in June of 1991, 18 months later, suggested a phase reversal of the EDJs (Böning and Schott 1993). A numerical model simulation failed to reproduce the short vertical wavelength of the EDJs, but it suggested that larger-vertical-scale equatorial current reversals at depth might be due to an annual Rossby wave (Böning and Schott 1993).

Float observations suggested a complicated system of reversing zonal flows around the equator with a mix of short and longer vertical scales, long zonal scales, short meridional scales, and timescales on the order of a year or more. Six SOFAR floats deployed at 800 m moved eastward between 5°S and 6°N, with a mean speed of 0.11 m s^{-1} for about their first 17 months (Richardson and Schmitz 1993). Three of the four floats still in this latitude band reversed direction for the next four months to move westward. The authors recognized that these sparse data had a strong potential for aliasing reversals of zonal currents with short meridional scales. SOFAR floats at around 1800 m near the equator moved eastward for the first 13 months of their mission and then westward for the next 8 months, with mean speeds around 0.04 m s^{-1} in either direction. However, floats north of 1°N moved in the overall opposite direction from those on the equator during this time (Richardson and Schmitz 1993). Over the full 3.7-yr mission of these 1800-m-depth floats, the six trajectories in the region gave an overall suggestion of predominantly eastward flow centered near 2°S and 2°N and weaker westward flow centered near the equator (Richardson and Fratantoni 1999), but not without occasional flow reversals. However, these SOFAR floats inadvertently sank at a rate of about 135 m yr^{-1}, a behavior with potential to confuse vertical and zonal phase propagation of the EDJs, as discussed in section 5. A year of Profiling Autonomous Lagrangian Circulation Explorer (PALACE) float trajectories at 1000 m (Molinari et al. 1999) suggested zonal flows with speeds of about 0.15 m s^{-1}, long zonal scales, timescales of about a year, and zonal flows of opposite sign on the equator relative to those north of 2°N at any given time. The authors concluded that these patterns suggested the presence of equatorial Rossby waves.

Meridional sections of velocity profiles and CTD data with high vertical and meridional resolution have also helped to flesh out the description of the EDJs. Initial work using zonal velocity sections showed a 400–600-m vertical wavelength, meridional trapping within ±1.5° of the equator, and peak velocities on the order of 0.2 m s^{-1} centered near 1500-dbar pressure and prompted speculation on seasonal phase reversals in the EDJs (Gouriou et al. 1999). Three sections occupied at 35°, 23°, and 10°W during a single cruise showed that the EDJs extended across the entire basin from 500 to 2500 m, although they were not in phase at those three longitudes (Gouriou et al. 2001). In that study, predominantly eastward currents near 2°S and 2°N that appeared to encircle the EDJs were named the extra-equatorial jets (EEJs). Zonal velocity profiles from eight cruises were used to demonstrate strong zonal coherence of the EDJs over the 1000-km distance between 35° and 44°W (Send et al. 2002), with perhaps a slight vertical phase shift over that distance. In that study, data from a 20-month current meter mooring deployment of four instruments spaced evenly over about an EDJ vertical wavelength were analyzed to suggest that the EDJs remained nearly steady in amplitude and phase for at least a year. However, phase information over the 7-yr interval spanned by the eight cruises and the mooring deployment also suggested a potential for longer periodicity, perhaps on the order of 5 years or more (Send et al. 2002).

Historical CTD data have been used in the Pacific to show the EDJs in the eastern Pacific manifested themselves as a significant energy peak in vertical strain at 400-sdbar (stretched decibar) vertical wavelength on the equator with significant temporal coherence over two decades, significant zonal coherence over 5000 km, phase propagating downward at 13 sdbar yr^{-1}, and a very long zonal scale not distinguishable from zonal invariance (Johnson et al. 2002). The vertical, meridional, temporal, and zonal properties of these Pacific EDJs were broadly consistent with equatorial Kelvin wave dynamics. Here a similar analysis is performed, suggesting that some, but not all, of the Atlantic EDJ characteristics are broadly consistent with first-meridional-mode equatorial Rossby wave dynamics.

2. Data and processing

In the World Ocean Database 2001, 1274 CTD stations having no data gaps of greater than 20 dbar and reaching at least 1500-dbar pressure are available within ±8.25° of the equator in the Atlantic (Stephens et al. 2002), with 1068 of these reaching at least 2987 dbar (Fig. 1). These data, collected from 1972 through 1998, originate from a wide variety of programs. The 1990s World Ocean Circulation Experiment repeat sections at 35° and 44°W, often occupied sequentially on the same cruise (Send et al. 2002), are vital to the analysis. The Atlantic boasts mostly meridional sections with closely spaced full-depth CTD stations, concentrated in the western end of the basin. In contrast, eastern-Pacific deep CTD stations have been taken sparsely in space but frequently in time during Tropical Atmosphere–Ocean Array mooring maintenance cruises (Johnson et al. 2002).

The CTD processing closely follows Johnson et al. (2002). In brief, temperature and salinity are filtered and subsampled at 10-dbar intervals and then are used to

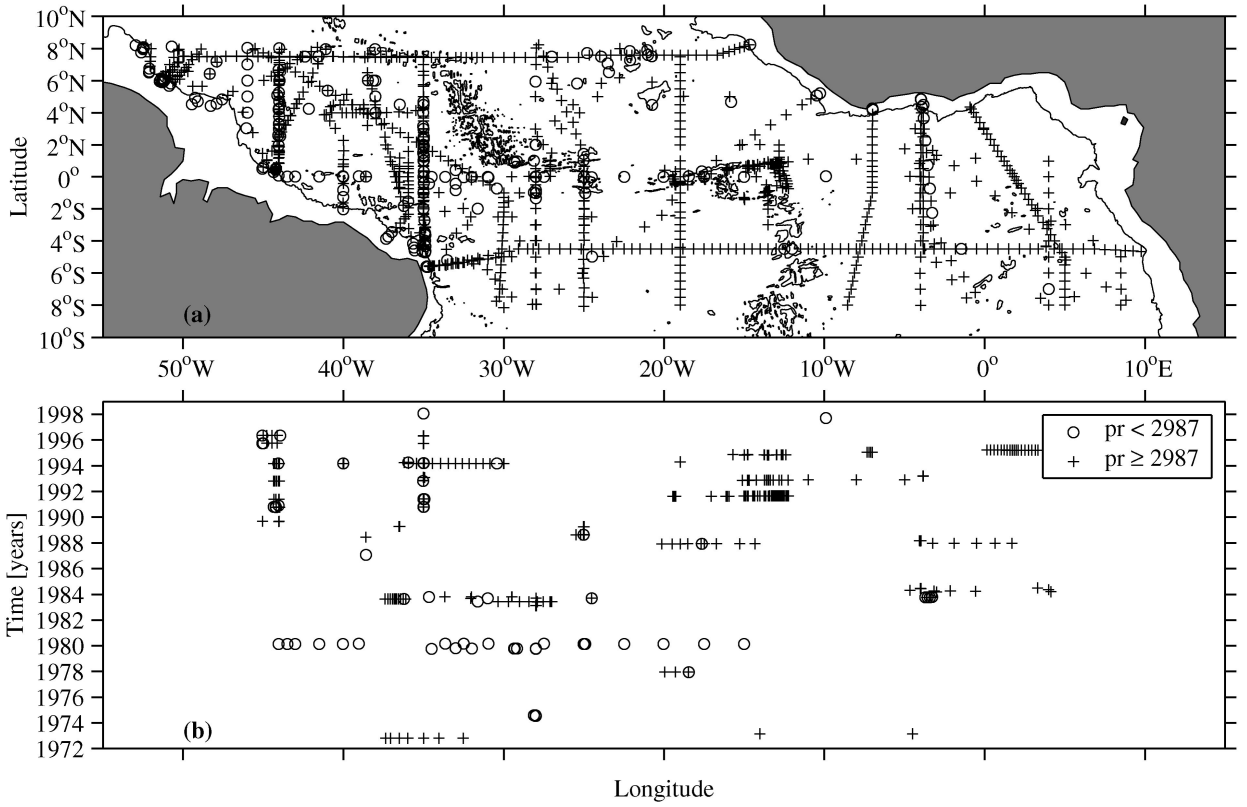

FIG. 1. (a) Latitude–longitude map of deep CTD stations. The 3000-m isobath (solid line) is from the General Bathymetric Chart of the Oceans (GEBCO) Digital Atlas published by the British Oceanographic Data Centre on behalf of the Intergovernmental Oceanographic Commission and the International Hydrographic Organisation in 1994. (b) Longitude–time map of all CTD stations within ±2.75° of the equator. Stations reaching to at least 1500 dbar but not 2987 dbar (open circles) are differentiated from those extending to or beyond 2987 dbar (pluses).

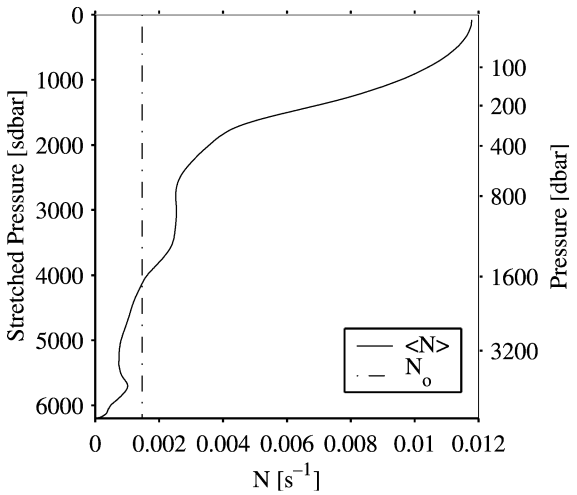

FIG. 2. The $\langle N \rangle$ (s^{-1}) profile (solid line) plotted against stretched pressure (sdbar), with reference unstretched pressures (dbar) on the right-hand side; N_0 (dash–dot line) is shown for reference.

estimate buoyancy frequency squared, $N^2 = -(g/\rho)(\partial\rho/\partial z)$, by centered differences over 20-dbar spans. Here g is the acceleration of gravity, z is the vertical axis (depth), and ρ is the potential density referenced to a local central pressure. Depth-varying background stratification results in changing wavelengths and amplitudes as the background stratification changes with depth. Wentzel–Kramers–Brillouin–Jeffreys (WKBJ) scaling and stretching (Leaman and Sanford 1975) compensate for the effects of varying stratification in the vertical by stretching the vertical coordinate system and scaling the signal amplitudes. After WKBJ scaling and stretching, variations of wavelength and amplitude owing to vertical variations in stratification are minimized, allowing identification of waves using standard spectral methods.

Mean vertical profiles of $\langle N \rangle$ (Fig. 2) and $\langle N^2 \rangle$ required for WKBJ stretching and scaling (Leaman and Sanford 1975), respectively, are estimated by averaging values at each pressure from all available CTD profiles within ±8.25° of the equator regardless of latitude, longitude, and time. These mean profiles are then smoothed vertically with a 39-point (200-dbar half-width) Hanning filter. WKBJ scaling is applied using the $\langle N \rangle$ profile to obtain stretched pressure $p^* = (1/N_0)(\int_0^p \langle N \rangle \, dp')$,

from pressure, with a reference $N_0 = 1.47 \times 10^{-3}$ s^{-1} chosen to be the vertical mean of $\langle N \rangle$, so the ranges of the stretched and unstretched pressures are identical. Stretched and unstretched pressures have equivalent vertical scales where $\langle N \rangle = N_0$, in this case near 1700-dbar (4125 sdbar) pressure.

The analysis here focuses on the water column between 374 and 2987 dbar (1950 and 5050 sdbar), a region between the thermocline and the sill depths of deep basins, within which N does not vary much horizontally. Although the sill depths of the deep basins are deeper than the analysis depth range, the near-equatorial Mid-Atlantic Ridge still has a considerable presence at 3000 m (Fig. 1a), but only in a few small isolated locations is the midocean bathymetry shallower than 2000 m.

Vertical strain, $\xi_z = (N^2 - \langle N^2 \rangle)/(\langle N^2 \rangle)$, is closely related to N^2 and reveals stretching and squashing of the density field. The raw ξ_z profiles are estimated from the original 10-dbar centered-difference N^2 profiles and $\langle N^2 \rangle$. These raw ξ_z profiles are transformed from their original uniform 10-dbar pressure grid to a uniform 10-sdbar stretched pressure grid. For the quantitative analysis (interpolated ξ_z), the raw values are linearly interpolated where $\langle N \rangle > N_0$. Where $\langle N \rangle < N_0$, so simple linear interpolation would alias short-wavelength information, the raw values are smoothed minimally during interpolation to preserve the energy for vertical wavelengths of 20 sdbar and longer.

3. Qualitative description

Because the EDJs are equatorially trapped and in geostrophic balance (Eriksen 1982; Muench et al. 1994), stretching and squashing of the density field on the equator correspond to zonal velocity anomalies. An equatorial Kelvin wave's ξ_z signature is largest on the equator (Fig. 3a). In this case, stretching is associated with eastward velocities, analogous to the Equatorial Undercurrent, and squashing corresponds to westward velocities, analogous to the Equatorial Intermediate Current. A first-meridional-mode equatorial Rossby wave has off-equatorial maxima of ξ_z (Fig. 3b). In this case, off-equatorial squashing is associated with equatorial eastward velocities, and stretching corresponds to equatorial westward velocities. There are zonal velocity nodes near the off-equatorial ξ_z maxima with poleward sign reversals in zonal velocity. Thus, it is possible to use ξ_z to help to distinguish between equatorial Kelvin waves and first-meridional-mode equatorial Rossby waves (Fig. 3). In addition, whereas equatorial Kelvin waves have equipartitioned equatorial maxima in zonal kinetic energy and available potential energy, equatorial Rossby waves have available-potential-energy off-equatorial maxima that are smaller than their zonal-kinetic-energy equatorial maximum (Moore and Philander 1977).

The meridional–vertical characteristics of the EDJs are illustrated with two well-sampled meridional–vertical sections at 35°W (Fig. 4). These sections use ξ_z profiles that are vertically smoothed using a loess (locally weighted polynomial regression and scatterplot smoothing) filter with a half-power point at 200 sdbar, which does not significantly affect the dominant EDJ vertical wavelength around 661 sdbar quantified in section 4. These vertically smoothed ξ_z profiles are used for illustrative purposes only here in section 3. Because ξ_z is prewhitened, sections of vertically smoothed ξ_z profiles allow a visual focus on the EDJ vertical wavelength, by removing much of the shorter-wavelength energy.

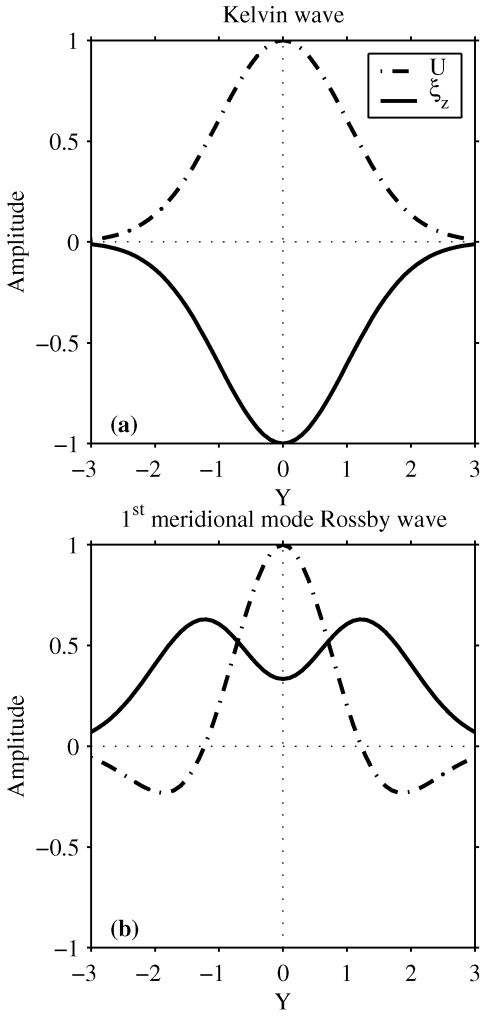

FIG. 3. Schematic of zonal velocity (U, dot–dashed line) and vertical strain (ξ_z, solid line) signatures for (a) an equatorial Kelvin wave and (b) a first-meridional-mode equatorial Rossby wave.

Overall, these sections are similar in appearance to those of mode-filtered zonal velocity for the same cruises (Fig. 3 of Send et al. 2002). The EDJ vertical wavelength around 661 sdbar is evident. The maximum ξ_z amplitude is located near 1200-dbar (3468 sdbar) pressure. Near-equatorial intensification of energy at these longer wavelengths is immediately visible in both sec-

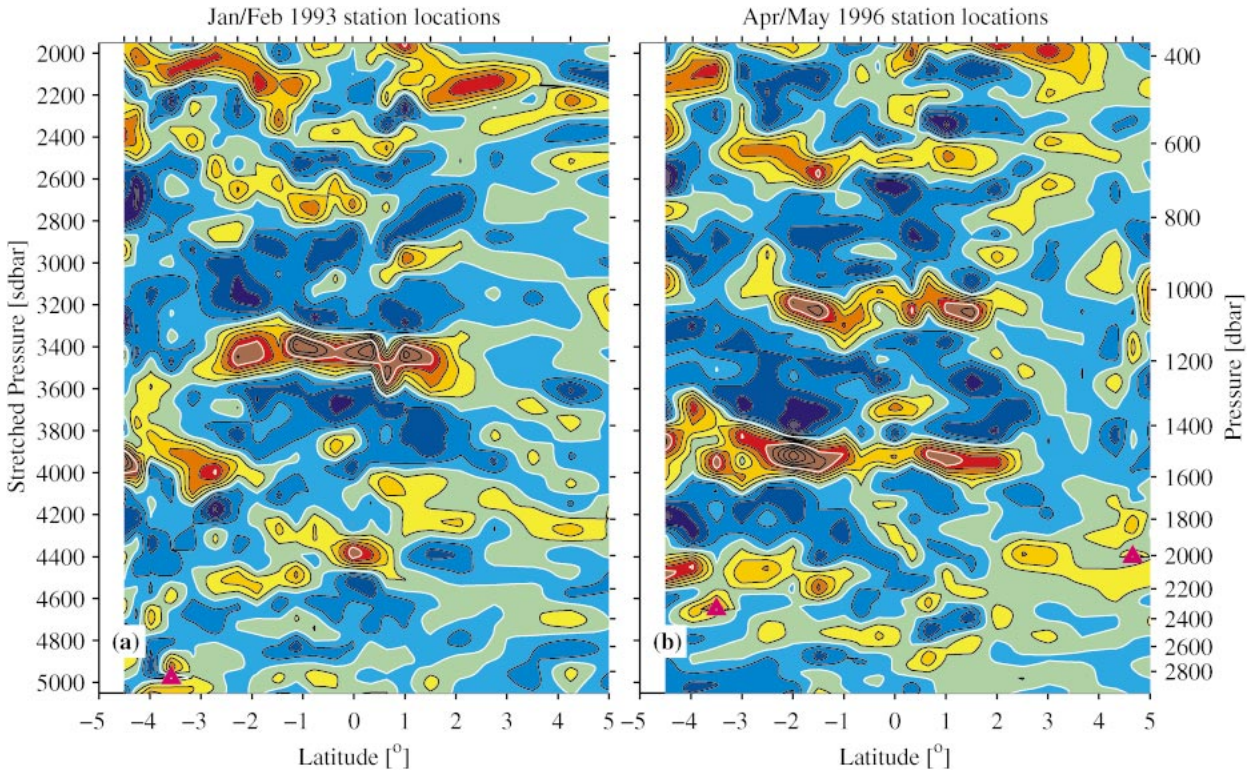

FIG. 4. Meridional–vertical sections of smoothed ξ_z at 35°W during (a) Jan–Feb 1993 and (b) Apr–May 1996. Negative values are blue and positive values are red, with black contours at 0.2 intervals (and white contours at integer values). CTD station locations are shown on panel tops. Magenta triangles indicate maximum pressures of profiles ending above or near 2987 dbar (5050 sdbar). Vertical axis is stretched pressures (sdbar), with reference unstretched pressures (dbar) on the right-hand side.

tions, with energy much reduced poleward of ±2.5°, especially at the northern end of the sections. The southern end of these sections is very close to the continental slope (Fig. 1a), so interaction among the deep-western boundary current, planetary waves, and the topography may contribute to the relatively high energy levels there. One qualitative difference between zonal velocity and ξ_z is that the EDJ zonal velocity has maximum amplitude very close to the equator, but ξ_z has maxima located about 1°–2° from it, near where EDJ zonal velocity has meridional nodes. In addition, careful comparison of zonal velocity (Fig. 3 of Send et al. 2002) and ξ_z (our Fig. 4) shows that off-equatorial stretching is associated with westward velocity on the equator. All of these characteristics of the Atlantic EDJs are reminiscent of first-meridional-mode equatorial Rossby waves, rather than equatorial Kelvin waves (Fig. 3).

4. Quantitative analysis

Studies summarized in section 1 have shown that the EDJs in the Atlantic are evident as near-equatorial features of several-hundred-decibar vertical wavelength existing perhaps from pressures of 500 to 2500 dbar, with an amplitude maximum near the center of that range. Wavelet analysis (Torrence and Compo 1998) is ideally suited to examining energy and phase of such localized features. Here, we use wavelet analysis on the data over a vertical range that exceeds that previously suggested for the EDJs to study quantitatively the EDJs using ξ_z profiles. We quantify the structure of the ξ_z field as a function of latitude, pressure, and vertical wavelength in the equatorial Atlantic. Our analysis suggests the EDJ signature near a vertical wavelength of 661 sdbar is strongest near ±1.5° from the equator and at 1232-dbar (3520 sdbar) pressure. The sparse zonal and temporal distribution of data (Fig. 1b) suggests long zonal and temporal scales, the latter being consistent with previous analyses of zonal velocity (Send et al. 2002). Together the zonal, temporal, and vertical scales are grossly consistent with first-meridional-mode equatorial Rossby waves.

The following analysis focuses on data from the 736 CTD stations that reach to at least 2987 dbar (5050 sdbar) equatorward of ±5.25°, and the middle portion of the water column, 374–2987 dbar (1950–5050 sdbar). This 3100-sdbar interval is in the portion of the water column within which $\langle N \rangle$ has minimal horizontal variations, and it encompasses the EDJ vertical range. Instead of the vertically smoothed ξ_z profiles discussed qualitatively in section 3, the interpolated ξ_z profiles, which resolve energy to near 20-sdbar wavelengths, are

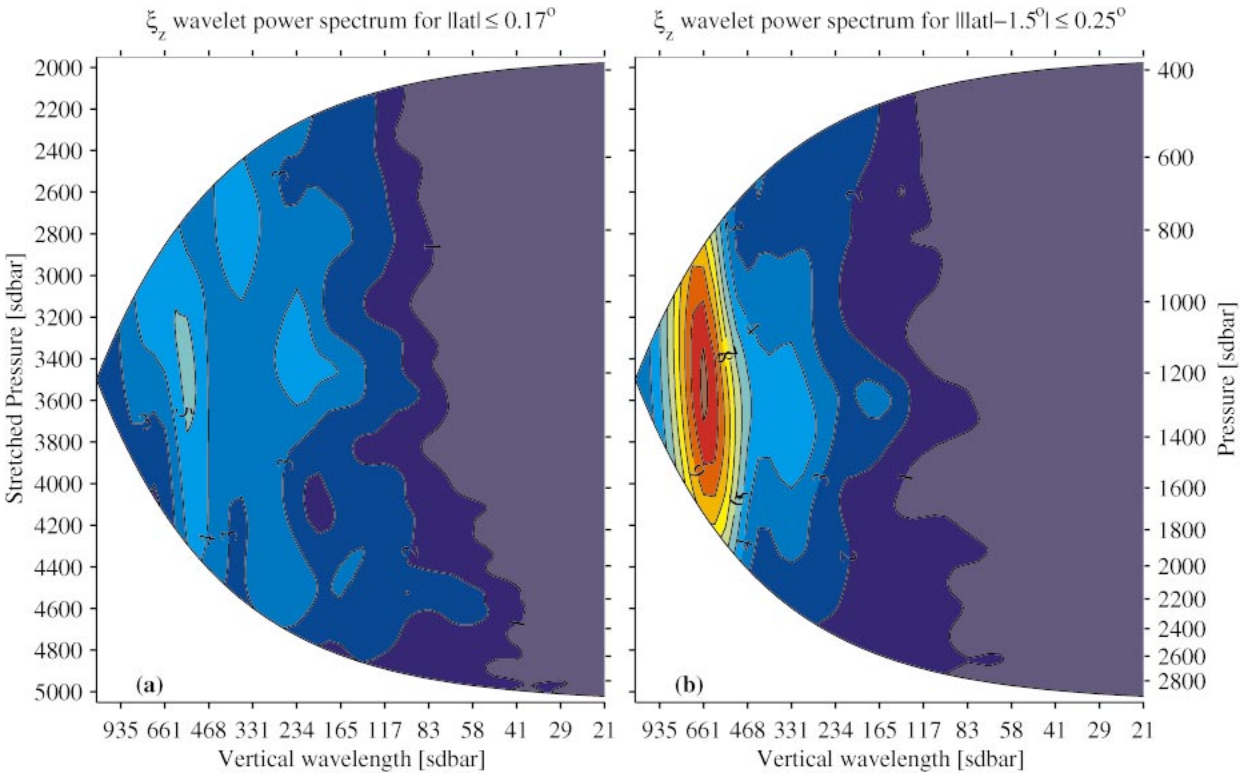

FIG. 5. Mean vertical wavelength wavelet power spectra of ξ_z using data between 374 and 2987 dbar (1950 and 5050 sdbar) from all CTD stations within (a) ±0.17° of the equator and (b) ±0.25° of ±1.5° from the equator. Contour interval for variance is $1.0\sigma^2$, where individual CTD stations have been normalized by the mean variance of all 1068 profiles reaching to at least 2987 dbar (5050 sdbar) within ±8.25° of the equator.

used in all the analysis that follows. Because ξ_z is a normalized, prewhitened quantity, no preparation is necessary for the wavelet analysis. A Morlet wavelet, essentially a Gaussian-modulated plane wave (Torrence and Compo 1998), is used for the wavelet function. The Morlet wavelet is very similar to a previous ad hoc model of the Atlantic EDJ structure (Send et al. 2002). The individual records are zero padded to limit edge effects. Results are blanked out where edge effects from the zero padding become potentially important. The spectra are normalized by the mean variance of all 1068 profiles reaching to at least 2987 dbar (5050 sdbar) within ±8.25° of the equator.

Mean wavelet power spectra of ξ_z are constructed as a function of latitude to reveal the meridional and vertical EDJ structure. These means result from averaging the data in non-overlapping bins based in part on the data distribution and centered at 0°, ±0.33°, ±0.67°, ±1°, ±1.5°, ±2°, . . . , ±5°. The equatorial bin (Fig. 5a) shows a peak exceeding 5 near 556-sdbar vertical wavelength and 1195-dbar (3460 sdbar) pressure. The ±1.5° bin (Fig. 5b) has the strongest peak of over 11 near 661-sdbar vertical wavelength and 1232-dbar (3520 sdbar) pressure. By the ±3.5° bin (not shown), all values of the power spectra lie below 1 and peaks are not obvious.

The meridional structure of the EDJs can be quantified by plotting the mean power of the 661-sdbar vertical wavelength at 1232-dbar (3520 sdbar) pressure in each latitude bin as a function of latitude (Fig. 6). Poleward of ±3.5° energy levels drop off to very low values. Equatorward, energy levels build to a maximum near ±1.5° before dropping somewhat toward the equator (but still remaining well above poleward background levels at the equator). As previously noted, this pattern is reminiscent of a first-meridional-mode equatorial Rossby wave (Fig. 3b).

The appropriate structure for the energy of a first-meridional-mode equatorial Rossby wave assuming a uniform background energy level a is $a + b\{[1 + 2(y/l)^2] \exp[-0.5(y/l)^2]\}^2$, where the Rossby wave energy level is b, and the meridional scale is l. A weighted nonlinear fit of this function to the data treating all three parameters as free yields a curve that sits within the 95% confidence intervals of nearly all of the means in latitudinal bins (Fig. 6, solid line), with $l = 1.1°$. Unfortunately, although for linear Rossby waves in the presence of background noise it is legitimate to allow a and b to vary, l is not really a free parameter, being given by $l = (c/\beta)^{0.5} = 0.74°$, where $\beta = 2.3 \times 10^{-11}$ m^{-1} s^{-1} is the meridional derivative of the Coriolis parameter, $c = (\lambda_z N_0)/(2\pi) = 0.15$ m s^{-1} is the Kelvin wave phase speed, and λ_z is the vertical wavelength.

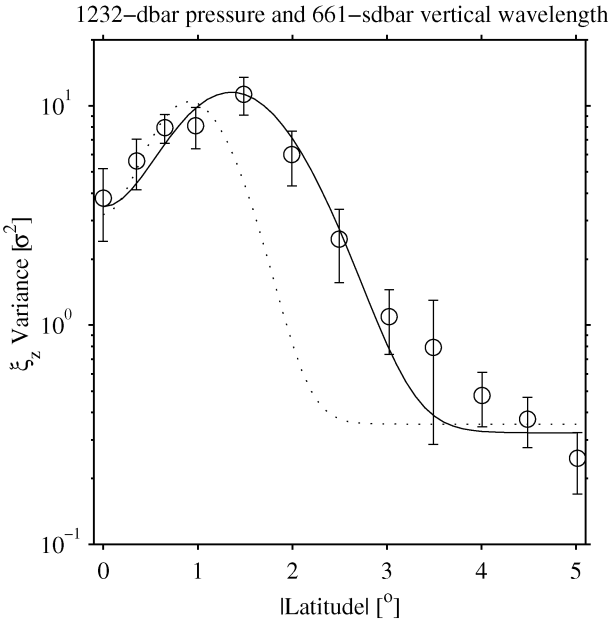

FIG. 6. Mean variance as a function of latitude at 661-sdbar vertical wavelength and 1232-dbar (3520 sdbar) pressure from wavelet power spectra of ξ_z as a function of latitude (open circles). Two standard errors of the mean (error bars) give roughly 95% confidence intervals, given the assumption that each CTD station is independent. Fits of first-meridional-mode equatorial Rossby wave energy structure with uniform background energy levels fixing the meridional scale at the theoretical value (dotted line) or allowing the meridional scale to vary (solid line) are shown.

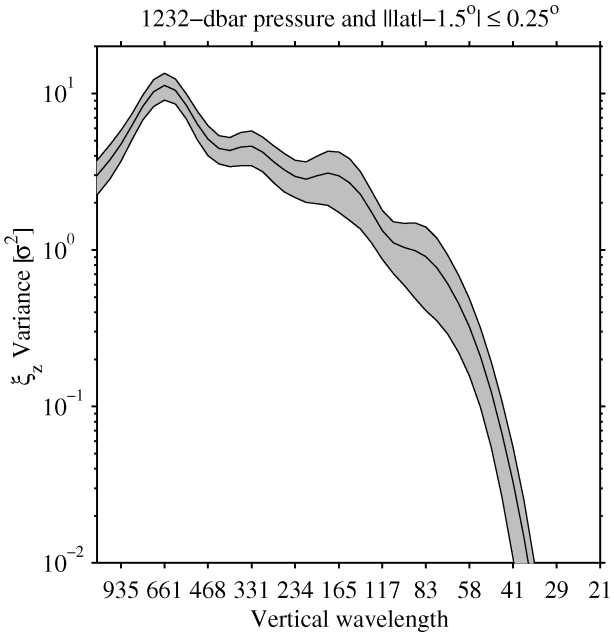

FIG. 7. Mean vertical wavelength wavelet power spectrum of ξ_z at 1232-dbar (3520 sdbar) pressure using data between 374 and 2987 dbar (1950 and 5050 sdbar) from stations within $\pm 0.25°$ of $\pm 1.5°$ from the equator (solid line). Two standard errors of the mean (shading) give roughly 95% confidence intervals, with the assumption that each CTD station is independent.

The best-fit meridional scale is 1.5 times the theoretical value. When the same model is applied with l fixed at the theoretical value, the resulting fit (Fig. 6, dotted line) is poor.

A cut across the wavelet spectrum at $\pm 1.5°$ at 1232-dbar (3520 sdbar) pressure shows the finite width of the EDJ spectral peak (Fig. 7). Using the vertical wavelengths at which the variance of that peak drops to half-maximum for estimates of the EDJ vertical wavelength uncertainty gives 485 sdbar $< \lambda_z <$ 889 sdbar. Even with this conservative error estimate, the range of theoretically predicted Rossby wave meridional scale is $0.63° < l < 0.86°$. These values are well below the best fit to the observations of $l = 1.1°$.

Similarly broad meridional scales were found previously for the EDJs in the central Pacific, and an explanation was advanced that meridional advection by higher-frequency meridional motions might smear out the EDJ signature if aliased by infrequent sampling (Muench et al. 1994). Another plausible mechanism for meridional-scale changes, which may be significant at some depths in the Pacific, is modification of β by curvature in the zonal velocity field of background currents or the EDJs themselves (Hua et al. 1997). Such nonlinearities can change the theoretical meridional scale and zonal wavelength of equatorial waves (Philander 1979). However, the deep zonal flows in the Atlantic are not sampled sufficiently well to investigate this hypothesis.

A previous investigation (Weisberg and Horigan 1981) suggested nonlinearity of the EDJs might be anticipated because zonal velocities, on the order of 0.1–0.2 m s^{-1} (Gouriou et al. 1999, 2001; Send et al. 2002), are similar in magnitude to the Kelvin wave phase speed of 0.15 m s^{-1} and are larger than the first-meridional-mode Rossby wave phase speed of one-third of this value. However, this condition by itself does not guarantee nonlinearity, which would have to involve phenomena such as standing waves or wave mean-flow interaction.

Harmonic peaks, typical of large-amplitude structures, are revealed by a cut across the wavelet spectrum at $\pm 1.5°$ and 1232-dbar (3520 sdbar) pressure (Fig. 7). As previously noted, the strongest peak is around 661-sdbar vertical wavelength. However, peaks of decreasing strength are obvious near vertical wavelengths of 331 and 180 sdbar, with a plateau around 83 sdbar. These values correspond to wavelengths of 1/2, 1/4, and 1/8 of the primary vertical wavelength. Although the shortest harmonic is only a plateau and the others do not rise above 95% significance, the overall pattern is clear. Similar harmonic patterns are repeated in the other energetic latitude bins (not shown). The structure associated with these harmonics is evident in the ξ_z sections (Fig. 4). Squashing (positive values) has larger amplitude and smaller vertical scale while stretching (negative values)

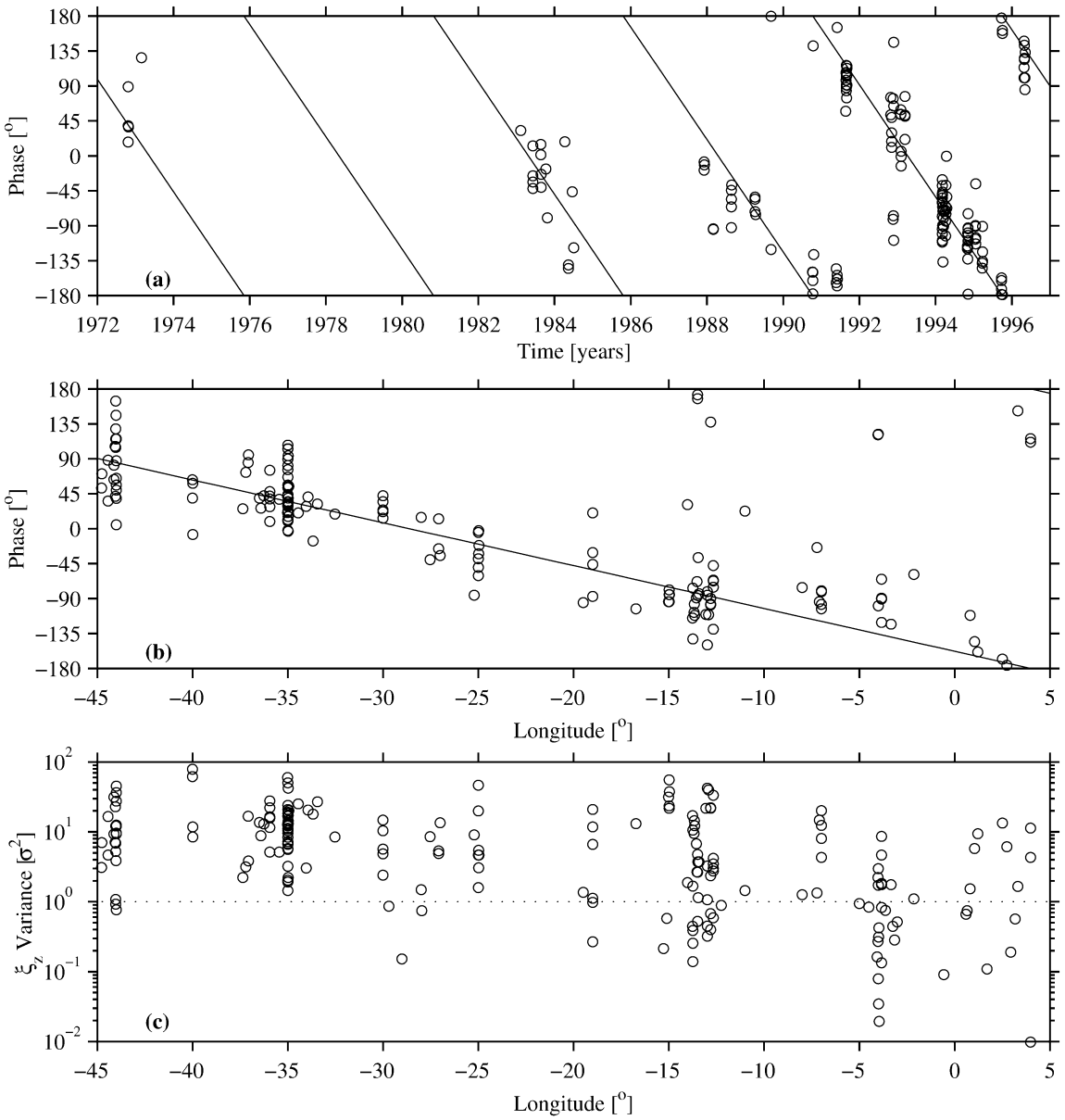

FIG. 8. Data at 661-sdbar vertical wavelength and 1232-dbar (3520 sdbar) pressure from stations greater than ±0.83° and less than ±2.25° from the equator. (a) Phase (circles) with zonal periodicity removed plotted against time with least squares estimate of 5-yr temporal periodicity (solid line). Only phases associated with variance greater than unity are used. (b) Phase (circles) with temporal periodicity removed plotted against longitude with least squares estimate of 70° zonal periodicity (solid line). Only phases associated with variance greater than unity are used. (c) Variance of ξ_z (circles) plotted against longitude with cutoff level of unity (dotted line) employed for estimates of zonal wavelength and period.

has smaller amplitude and larger vertical scale. These harmonics are probably an artifact of working in pressure, rather than density, coordinates (E. Kunze 2002, personal communication).

Spatial and temporal sampling (Fig. 1) are fairly sparse for quantification of zonal and temporal scales using phase information. Nonetheless, we analyze phase estimates for ξ_z derived from the wavelet analysis of individual CTD stations, using phase for the 661-sdbar vertical wavelength and 1232-dbar (3520 sdbar) pressure from the three most energetic longitude bins: ±1°, ±1.5°, and ±2°. We retain only phase data with normalized variance exceeding unity at this vertical wavelength and pressure (values above the dotted line in Fig. 8c, 160 of the 203 estimates, or 79%). Thus, potentially noisy phase estimates where the EDJ signature is weak are discarded. Each retained phase estimate is associated with a time between 1972 and 1996 and a longitude between 45°W and 5°E (Figs. 8a,b).

Fitting these phase estimates to a sinusoidal function

of time and longitude yields a period T and zonal wavelength λ_x that minimize phase variance. A clear minimum in phase variance exists for a 5 ($\pm$1) yr period (Fig. 8a) and a 70° ($\pm$60°) zonal wavelength (Fig. 8b), with uncertainties being two standard errors of the mean, for roughly 95% confidence intervals. Given the long zonal and temporal scales of the EDJs, the individual phase estimates are clearly not all independent. To estimate the effective number of independent samples for the confidence intervals quoted above, we assume a Gaussian covariance structure with zonal and temporal decorrelation scales of $\lambda_x/(2\pi)$ and $T/(2\pi)$, respectively. These assumptions suggest the 160 phase estimates are equivalent to about 18 independent samples.

Assuming the previously estimated conservative range of EDJ vertical wavelengths from 485 to 661 sdbar through 889 sdbar together with the period of 5 ($\pm$1) yr estimated from the data, the theoretically predicted zonal wavelength for a first-meridional-mode equatorial Rossby wave is $\lambda_x = (c/3)T = 70°$ ($\pm$30°). The theoretical value agrees well with the estimate above from observations. If one assumes that linear wave dynamics hold, the downward phase propagation, also found in the Pacific (Johnson et al. 2002), implies upward energy propagation. However, neither vertical nor zonal energy propagation is evident in the variance vertical maxima. This lack is inconsistent with linear wave dynamics. The only discernible pattern in the variance magnitudes at this vertical wavelength, pressure, and latitude range is that they appear to grow to the west (Fig. 8c).

5. Discussion

Vertical strain ξ_z is analyzed across the middepth equatorial Atlantic Ocean using CTD data, predominantly from the 1990s (Fig. 1). As noted previously for zonal velocity (Gouriou et al. 1999, 2001; Send et al. 2002), the peak in ξ_z energy is found around 661-sdbar vertical wavelength and 1232-dbar (3520 sdbar) pressure (Fig. 5). Off-equatorial maxima in ξ_z at the EDJ vertical wavelength are revealed (Fig. 6). These maxima occur at the same latitudes, roughly $\pm$1.5°, as nodes in zonal velocity apparent in published zonal velocity sections but not previously discussed. This ξ_z and zonal velocity structure is grossly consistent with first-meridional-mode equatorial Rossby waves (Fig. 3), but the meridional length scale is about 1.5 times the theoretical prediction. This discrepancy may be the result of nonlinearities induced by strong low-frequency zonal currents (Hua et al. 1997) or aliasing of vigorous high-frequency meridional advection (Muench et al. 1994). In addition, observed EDJ zonal velocities are strong—matching, or even exceeding, the Kelvin wave phase speed of 0.15 m s^{-1}. The harmonic peaks found at 1/2 and 1/4 of the EDJ vertical wavelength (Fig. 7) are typical of large-amplitude features. Downward phase propagation with a 5 ($\pm$1) yr period at the EDJ vertical wavelength is found (Fig. 8), as previously speculated using data spanning a shorter time period (Send et al. 2002). In addition, a zonal wavelength of 70° ($\pm$60°) is estimated for the Atlantic EDJs. The vertical, time-, and zonal scales of the Atlantic EDJs together are roughly consistent with first-meridional-mode equatorial Rossby wave dynamics.

The generation mechanism for the EDJs is not determined here. The 5 ($\pm$1) yr period coupled with a vertical wavelength around 661 sdbar suggests a downward phase propagation of about 132 ($\pm$12) m yr^{-1}. Wave theory suggests upward energy propagation, but such upward propagation is not discernible in the variance vertical maxima. However, given their slow vertical phase speeds, it would be very difficult for the EDJs to propagate upward from some remote forcing near the bottom as linear waves and to maintain strength in the presence of dissipation (Muench and Kunze 1999, 2000). The EDJ middepth variance maximum and increasing variance to the west are also not in accord with the idea of remotely forced linear waves. As an alternative, the EDJs may be generated locally by an equatorial inertial instability (Hua et al. 1997), perhaps triggered by some combination of background currents and annual Rossby waves. Deposition of momentum at critical layers by the internal wave field might then help to maintain the jets in the face of dissipation (Muench and Kunze 1999, 2000). Forced and dampled thusly, the EDJs could still roughly conform to linear equatorial wave dynamics, as they appear to do in everything but their too-broad meridional scale and the apparent lack of upward propagation in the variance vertical maxima.

A curious finding is that the sinking rate of about 135 m yr^{-1} inherent in some SOFAR floats deployed in the region (Richardson and Schmitz 1993; Richardson and Fratantoni 1999) almost perfectly matches the EDJ vertical phase velocity. This accident could make time-reversing flows induced by vertical phase propagation of the EDJs look like unidirectional flows when sampled by the sinking SOFAR floats, leading to potentially erroneous conclusions about the nature of the equatorial circulation in the equatorial Atlantic. In addition, the very long timescale of the EDJs requires a longer time series than the 3.7-yr float records to resolve.

The EDJs do not exist in isolation. There are other circulation features with longer meridional and vertical scales and unknown timescales, such as the EEJs that surround the EDJs (Gouriou et al. 2001). Numerical model analysis (Böning and Schott 1993) and profiling float trajectories (Molinari et al. 1999) suggest wind-driven annual Rossby waves, likely with longer vertical scales than the EDJs, reach the depths of the EDJs. The deep western boundary current passes through the region (Gouriou et al. 2001; Richardson and Fratantoni 1999). Nonlinear interaction among these phenomena seems possible. Measurements taken with high meridional, temporal, and vertical resolution over long zonal

distances and long time spans may be required for complete analyses of these circulation features.

Acknowledgments. This work was funded by the NOAA Office of Oceanic and Atmospheric Research and the NOAA Office of Global Programs and was partially funded by the Joint Institute for the Study of the Atmosphere and Ocean (JISAO) under NOAA Cooperative Agreement NA17RJ1232. It would not have been possible without the careful and sustained work of the officers, crew, and scientific parties of the many international scientific programs involved in collecting deep CTD data in the equatorial Atlantic, especially French and German expeditions. Conversations with Dennis Moore and LuAnne Thompson were useful. Comments from Eric Firing, Eric Kunze, and two anonymous reviewers improved the manuscript.

REFERENCES

Böning, C. W., and F. A. Schott, 1993: Deep currents and the eastward salinity tongue in the equatorial Atlantic: Results from an eddy-resolving, primitive equation model. *J. Geophys. Res.,* **98,** 6991–6999.

Eriksen, C. C., 1982: Geostrophic equatorial deep currents. *J. Mar. Res.,* **40** (Suppl.), 143–157.

Gouriou, Y., B. Bourlès, H. Mercier, and R. Chuchla, 1999: Deep jets in the equatorial Atlantic Ocean. *J. Geophys. Res.,* **104,** 21 217–21 226.

——, and Coauthors, 2001: Deep circulation in the equatorial Atlantic Ocean. *Geophys. Res. Lett.,* **28,** 819–822.

Hua, B. L., D. W. Moore, and S. Le Gentil, 1997: Inertial non-linear equilibration of equatorial flows. *J. Fluid Mech.,* **331,** 345–371.

Johnson, G. C., E. Kunze, K. E. McTaggart, and D. W. Moore, 2002: Temporal and spatial structure of the equatorial deep jets in the Pacific Ocean. *J. Phys. Oceanogr.,* **32,** 3396–3407.

Leaman, K. D., and T. B. Sanford, 1975: Vertical energy propagation of intertial waves: A vector spectral analysis of velocity profiles. *J. Geophys. Res.,* **80,** 1975–1978.

Molinari, R. L., S. L. Garzoli, and R. W. Schmitt, 1999: Equatorial currents at 1000 m in the Atlantic Ocean. *Geophys. Res. Lett.,* **26,** 361–363.

Moore, D. W., and S. G. H. Philander, 1977: Modeling of the tropical ocean circulation. *The Sea,* E. D. Goldberg et al., Eds., Marine Modeling, Vol. 6, John Wiley and Sons, 319–361.

Muench, J. E., and E. Kunze, 1999: Internal wave interactions with equatorial deep jets. Part I: Momentum-flux divergences. *J. Phys. Oceanogr.,* **29,** 1453–1467.

——, and ——, 2000: Internal wave interactions with equatorial deep jets. Part II: Acceleration of the jets. *J. Phys. Oceanogr.,* **30,** 2099–2110.

——, ——, and E. Firing, 1994: The potential vorticity structure of equatorial deep jets. *J. Phys. Oceanogr.,* **24,** 418–428.

Philander, S. G. H., 1979: Equatorial waves in the presence of the Equatorial Undercurrent. *J. Phys. Oceanogr.,* **9,** 254–262.

Ponte, R. M., J. Luyten, and P. L. Richardson, 1990: Equatorial deep jets in the Atlantic Ocean. *Deep-Sea Res.,* **37,** 711–713.

Richardson, P. L., and W. J. Schmitz, 1993: Deep cross-equatorial flow in the Atlantic measured with SOFAR floats. *J. Geophys. Res.,* **98,** 8371–8387.

——, and D. M. Fratantoni, 1999: Float trajectories in the deep western boundary current and deep equatorial jets of the tropical Atlantic. *Deep-Sea Res.,* **46B,** 305–333.

Send, U., C. Eden, and F. Schott, 2002: Atlantic equatorial deep jets: Space–time structure and cross-equatorial fluxes. *J. Phys. Oceanogr.,* **32,** 891–900.

Stephens, C., and Coauthors, 2002: *Temporal Distribution of Conductivity/Salinity–Temperature–Depth (Pressure) Casts.* Vol. 3, *World Ocean Database 2001,* NOAA Atlas NESDIS 44, 47 pp. and CD-ROMs.

Torrence, C., and G. P. Compo, 1998: A practical guide to wavelet analysis. *Bull. Amer. Meteor. Soc.,* **79,** 61–78.

Weisberg, R. H., and A. M. Horigan, 1981: Low-frequency variability in the equatorial Atlantic. *J. Phys. Oceanogr.,* **11,** 913–920.